Co-Polyesters of Hydroxy-Fatty Acids Extracted from Tomato Peel Agro-Wastes and Glycerol with Tunable 16 Mechanical, Thermal and Barrier Properties

Mathilde Marc, Regis Risani, Eric Desnoes, Xavier Falourd, Bruno Pontoire, Rubens Rodriguez, Rita Escorcio, Ana Paula Batista, Romain Valentin, Nathalie Gontard, et al.

HAL Id: hal-02980994
https://hal.inrae.fr/hal-02980994v1

Preprint submitted on 27 Oct 2020 (v1), last revised 21 Dec 2020 (v2)

1   **Synopsis**

2

3   Bioinspired polyester elastomers synthesized from glycerol and tomato agrowaste, through a catalyst-

4   and solvent-free process display new and tunable properties.

5

6   **Graphical abstract**

7

8

9

10

11

12

13

14

Co-polyesters of hydroxy-fatty acids extracted from tomato peel agro-wastes and glycerol with tunable mechanical, thermal and barrier properties

Mathilde Marc[†], Regis Risani[†], Eric Desnoes[†], Xavier Falourd[†,¶], Bruno Pontoire[†], Rúben Rodrigues[&], Rita Escórcio[&] , Ana Paula Batista[‡], Romain Valentin[§], Nathalie Gontard[‡], Cristina Silva Pereira[&], Christelle Lopez[†], Eric Leroy[ꓞ], Denis Lourdin[†], Didier Marion[†], Bénédicte Bakan[†*].

[†] Biopolymers Interactions Assemblies Research Unit 1268 (BIA), INRAE, Rue de la Géraudière, 44316, Nantes, France

[‡] Agropolymers Engeneering and Emerging Technologies Joint Research Unit 1208 (IATE), INRAE-CIRAD-SupAgro-University of Montpellier, 2 place Viala, Montpellier, 34000, France

[§] Agro-Industrial Chemistry Joint Research Unit 1010 (LCA), INRAE-INP-ENSIACET, 4 Allée Emile Monso, Toulouse, 31000, France

[¶] Biopolymers and Structural Biology platform (BIBS), BIA research unit, INRAE, rue de la Géraudière, Nantes, 44300, France

[ꓞ] Université de Nantes. Oniris. CNRS. GEPEA. UMR 6144 44600 Saint Nazaire, France.

[&] Instituto de Tecnologia Química e Biológica António Xavier, Universidade Nova de Lisboa (ITQB NOVA), Av. da República, Oeiras, 2780-157, Portugal.

*corresponding author: benedicte.bakan@inrae.fr

Abstract

By mimicking the cutin natural polyester networks of plant cuticles, we produced hydrophobic elastomers by a sustainable process, i.e., using a catalyst- and solvent-free polycondensation of glycerol and hydroxy-fatty acids, two by-products of the agro-food industry. The hydroxy-fatty acid fraction was obtained by alkaline hydrolysis in ethanol of peels from industrial tomato pomaces. This industrial-like fatty acid fraction contained more than 90% wt. of 9(10)-16 dihydroxyhexadecanoic acid (diOHC16). The co-polyesters were designed by increasing the ratio of esterified glycerol/diOHC16 in a range observed in plant cutins (up to 6% wt.). Their structure and functional properties (thermal, mechanical, gas permeability, interaction with bacterial cells) were characterized. Increasing the glycerol contents induced a significant decrease in the reticulation degree of the polyesters and the formation of crystalline domains with an hexagonal organization. These structural modifications were related to a marked increase of elastomeric extensibility (up to 217%). While water vapor permeability was not impacted, the increase of glycerol content induced a significant decrease of oxygen permeability. None of the polyesters displayed biocide activity, but an increase of glycerol content significantly reduced the adhesion of bacterial cells, potentially giving rise to antifouling applications. Finally, the increasing content of free hydroxyl groups of the co-polyesters offer opportunities of grafting and covalent substitution for tailored functionalization.

Introduction

To face terrestrial life colonization, plants have developed a hydrophobic barrier, the cuticle, that covers the surface of every aerial organs. This ubiquitous interface between the plant and its environment, fulfils multiple crucial functions such as mechanical supports against wounding and cracks, control of non-stomatal water loss and permeation of gases[1].

The main biopolymer of this complex hydrophobic assembly is the cutin polyester, that is essential for the functional properties of the plant cuticle[2, 3]. Cutin is insoluble due to its polyester network architecture. It can be depolymerized mainly into a variety of long chain hydroxy-fatty acids building blocks. Each of these carboxylic acid monomers contains 16 and-or 18 carbon atoms and one to three hydroxyl groups. Interestingly, the tomato fruit peels concentrate high amount of cutin, whose monomer composition is strikingly homogenous, with more than 80% by weight consisting of 9(10)-16 dihydroxyhexadecanoic acid (diOHC16). These ω-hydroxylated molecule carrying midchain functionalities, present high interfacial properties [4], but constitutes also a unique opportunity for the development of innovative biosourced polymer materials from depolymerized tomato cutin feedstock [5]. Reaching this innovation would address the important landmarks set by the United Nations sustainable development goals because tomato cutin is a readily available residue of the tomato processing industries. Tomato wastes, i.e., pomaces, are mainly composed of peels and seeds. 44 MT of tomato fruit are processed worldwide, to make derived tomato products (e.g., purees, juice, sauces) generating nearly 1.5 MT of animal feed and production of biogas whereas their transformation for development of new materials, from bioplastic to high-functional value products remains largely overlooked [6]. Peels and seeds can be easily separated and dried, directly in the factory, and the hydroxy-fatty acids can be easily extracted from the cutin of tomato peels [7].

Furthermore, glycerol, a main by-product of the biodiesel and oil industries [8], has been identified as a potentially influent minor component in tomato cutin. Esterified glycerol has been evidenced in the cutin polyester network structure [9] and typically represents only 0.6 to 0.7 % wt. of the cutin monomers obtained by depolymerization (Philippe et al 2016). In addition, we have recently highlighted that the ratio of the glycerol to hydroxy-fatty acid can be modulated in tomato fruit. Indeed, in tomato fruit mutants affected in a cutin synthase (CUS1), an enzyme involved in the cutin biosynthesis, a 60% reduction in cutin deposition was induced without any significant negative impact either on the fruit development or the

94   generation of cracks [10]. Looking at the cutin polyester structure, we observed a significant increase of ratio

95   of the glycerol to hydroxy-fatty acid . These results obtained with the mutants suggested that the inclusion

96   of co-polymerized glycerol in the tomato cutin network could be involved in the mechanical adaptation of

97   the fruit cuticle, in particular in the modulation of its extensibility. This is especially essential for resistance

98   to turgor pressure during fruit growth and environmental constraints to prevent fruit from cracking, a

99   phenomenon responsible for major crop losses [12]. Taking inspiration from nature, our leading hypothesis

100   is that we can produce tunable bio-based co-polyesters that mimic potential adaptive events of cutin

101   simply by playing on the glycerol/diOHC16 ratio.

102   Hereinafter, we describe a solvent- and catalyst-free polymerization process to generate co-

103   polyesters elastomers from two diOHC16 and glycerol, two readily available and renewable biological

104   resources. Tuning of the ratio of esterified glycerol to diOHC16 in a range similar to what it is observed in

105   plant cutin effectively results in the modulation of the structure (amorphous or semi-crystalline), the

106   properties (mechanical, thermal and barrier properties) of the ensuing co-polyesters.

107
108
109   **Experimental Section**

110

111   **Materials**

112   Glycerol (99 % purity) and all other chemical ACS reagents were from Sigma-Aldrich (USA). The analytical

113   grade solvents were obtained from Carlo Erba (Val de Reuil, France). The 16-10(9)-hydroxy-hexadecanoic

114   acid enriched hydroxy-fatty acid fraction (referred as "diOHC16" in the manuscript) was extracted from

115   industrial tomato pomaces provided by the "Conserveries de Bergerac" (UNIPROLEDI, Bergerac, France).

116   The peels and seeds of the pomaces were separated by decantation in a water tank. The floating peels

117   were recovered, their water excess was squeezed out and then dried at room temperature. Dried peels

118   (1kg) were grounded and dewaxed under reflux of acetone: ethanol 1:1 (v:v) in a Soxhlet extractor and

119   then dried in a fume hood. Cutin depolymerization was conducted at room temperature in 5% (wt.) KOH

120   in ethanol 95%. After filtration on a Buchner funnel, about 90% of the filtrate was evaporated under

121   vacuum and replaced by water. Hydroxy-fatty acids were precipitated by adjusting pH at 3.5 with

122   concentrated HCl. The hydroxy-fatty acid precipitate was extensively washed with water, and finally

123   freeze-dried.

124   The purity of the fatty acids was determined after phase partitioning in $CHCl_3/CH_3OH/H_2O$ 8:4:3

125 (v:v). The lower chloroform-rich phase containing only lipophilic compounds, mainly fatty acids and some

126 pigments, was recovered, evaporated under vacuum and weighed. The cutin monomer batches contains

127 98 ± 0.5% of lipophilic compounds. The fatty acid composition of the lipophilic fraction was determined by

128 gas chromatography coupled to a mass spectrometer as previously described [13]. A 60% yield of hydroxy-

129 fatty acids was obtained and the same batch of 500g of diOHC16 extract was used in the study. This batch

130 was dark-red colored due to the remaining pigments and consisted of ~90 % diOHC16 (**Supplemental Table**

131 **1**).

132

133 **Preparation of the cutin-like co-polyesters films**

134 Co-polyesters films were produced by a solvent-free and catalyst-free polycondensation. We developed a

135 polymerization process in order to minimize the non-esterified glycerol within the copolyester films.

136 Preparation with different weight ratio of diOHC16/ Glycerol (1.8g diOHC16 for PG0.4 ; 1.71g diOHC16/90

137 mg glycerol for PG2.3; 1.62gdiOHC16/180 mg glycerol for PG3.9; 1.53g diOHC16/ 270 mg glycerol for

138 PG4.8 ; 1.44g diOHC16/ 360 mg glycerol for PG5.2 and 1.35 g of diOHC16/ 450 mg glycerol for PG6.2

139 respectively) were put in Teflon molds (5 cm x cm) with a thickness of about 0.7-1 mm. The nomenclature

140 of the co-polyesters refers to the glycerol weight ratio comprised within the co-polyester at the end of the

141 process (**Table 1**). Bulk poly-condensation was then conducted for 24h at 150°C in an oven (VaccuTherm,

142 ThermoFisher, USA). In order to avoid bubbles and to minimize the presence of residual free glycerol, i.e.,

143 non-esterified, in the final material a 400mbar vacuum was applied during the first 2h of the

144 polycondensation process. After 24h, the polymers were rapidly cooled on ice and stored at room

145 temperature. Samples of the ensuing films were immersed under agitation in various solvents of diOHC16

146 and/or of glycerol, i.e., water, ethanol and chloroform 16h at room temperature to assess their solubility.

147

148 **Structural characterization of the cutin-like co-polyester films**

149 Attenuated total reflectance Fourier-transform infrared spectroscopy (ATR-FTIR) spectra (200 scans) were

150 recorded at a resolution of 2 cm^{-1} on a Nicolet Magna IR 550 spectrometer equipped with a liquid nitrogen

151 cooled mercury–cadmium–telluride detector. The instrument was continuously purged with dry air.

152 Spectra of co-polyester films were obtained by attenuated total reflection (ATR) using

153 a single reflection accessory fitted with a thermostated diamond crystal with a 45° angle of light incidence.

154 All spectra (3 per co-polyester) were acquired in the 4000 to 700 cm^{-1} range at 4cm^{-1} resolution and

155 accumulating 30 scans.

156 ^{13}C solid state NMR (CP-MAS NMR) was carried out on a Bruker AvanceIII-400 MHz spectrometer

157 operating at 100.61 MHz for ^{13}C, equipped with a double-resonance H/X CP-MAS 4-mm probe for CP-MAS

158 (cross-polarization magic-angle-spinning) solid-state experiments. Sixty mg of the co-polyester films were

159 put packed into 4 mm zirconia rotors. The samples were spun at 12,000 Hz at room temperature. CP-MAS

160 spectra were acquired with a contact time of 1 ms, a recycling delay of 10 s and over accumulation of 2048

161 scans. The carbonyl carbon was set to 176.03 ppm through external glycine calibration. NMR spectra

162 deconvolution was performed using the PeakFit® software (Systat Software, Inc., USA).

163 X-Ray Diffraction analysis was performed on a Bruker-AXS D8 Discover diffractometer. The X-ray

164 beam was produced in a sealed copper tube at 40 kV and 40 mA. The 500-μm beam with a CuKα1

165 wavelength (1.5405 Å) was collimated and parallelized using two crossed-coupled Göbel mirrors. The X-

166 ray diffraction data were collected using a Vantec500 two-dimensional detector, previously calibrated with

167 silver behenate, in the 2.θ-range: 3-70°. The samples are placed perpendicular to the X-ray beam. Recorded

168 diffractograms I = f (2θ) were normalized to remove the influence of thickness variation among the

169 samples. Temperature kinetics were performed using Linkam's HFS91 stage. The samples were placed in a

170 mica window cell. The detector was positioned at a focusing distance of 8.6 cm from the sample surface.

171 It was in direct beam position. The heating kinetic applied to the sample was 3°C.min^{-1} from 20°C to 100°C.

172

173 **Chemical characterization of the cutin-like co-polyester films**

174 Free glycerol was extracted from polymers (5mg in 1 mL of CH$_3$OH), overnight at room temperature.

175 Esterified glycerol was released from polymers by mild methanolysis using a modified procedure [9]. Isolated

176 pieces of the co-polyester films were stirred at room temperature in a mixture of 50mM sodium methoxide

177 in dry methanol with the internal standard 1,2,3-butanetriol [14]. Free and esterified glycerol extracts were

178 dried with a nitrogen flow, and analyzed by GC-MS and GC FID. For the quantification of the cutin hydroxy-

179 fatty acids, the co-polyesters were depolymerized through methanolysis according to a described

180 procedure during 6h until complete depolymerization. The depolymerized hydroxy-fatty acids were

181 silylated with 1% BSTFA/TMCS and analyzed by GC-MS and GC-FID as previously described [11].

182   Free OH groups were derivatized by benzyl-etherification resistant to alkaline depolymerization,

183   according to an established method [11]. Briefly, co-polyesters (3mg) were mixed at 90°C in a screw-capped

184   glass tube for 24h with 15mg of 2-benzyloxy-1-methylpyridinium triflate and 1.68 mg of magnesium oxide

185   in 1mL of trifluorotoluene. The samples were then extensively washed with CH_2Cl_2 and dried before

186   depolymerization and cutin monomer analysis. GC-FID surface response of the labelled diOHC16 (either in

187   midchain position or in ω−position) were compared between the different co-polyesters and were

188   expressed as equivalent of heptadecanoic acid, as external standard.

189
190   **Thermal and mechanical properties of the cutin-*like* co-polyester films**

191   Differential Scanning Calorimetry (DSC) was performed on a DSC Q100 (TA Instruments, New Castle, DE,

192   USA). The DSC instrument was calibrated with an indium standard. Analyses were made with 2–5mg of

193   samples, using hermetically-sealed aluminium pans. An empty pan was used as a reference. Samples were

194   cooled from 20°C to −50°C and heated at $3°C.min^{-1}$ until 80°C. The Glass transition temperature (Tg) of the

195   co-polyesters was defined at the midpoint of heat capacity change on the thermograms recorded on the

196   first scan. The melting temperature was determined at the maximum of the peak.

197   Dynamic Mechanical Thermal Analysis (DMTA) was performed on a DMTA MKIV (Rheometric

198   Scientific, US). Rectangular specimens (20 mm ×4 mm) were cut from the films and thickness of about 0.7-

199   1 mm was precisely measured with a micrometer. The samples were analyzed in the tensile mode at the

200   frequency of 1 Hz with strain amplitude of 0.1%. To keep the samples taut a static force superior by 10%

201   to the dynamic force was applied to the sample. A scanning rate of $3°C min^{-1}$ from -50°C to 80 °C was used.

202   Each sample was analyzed in duplicate.

203   Tensile test of the films was carried out using MTS Synergie 100 (MTS Systems Corporation, USA).

204   The film samples were cut into a dog-bone shape. The test was performed using a cross-head speed of 10

205   mm/min. The reported results, including Young's modulus, ultimate strength and elongation at break,

206   were the average values of five specimens. The standard deviations are indicated in **Table 1**.

207
208   **Barrier properties of the cutin-like co-polyester films**

209   Water permeances of the co-polyesters were determined at 25°C and under 100% relative humidity

210   gradient using transpiration chambers as previously described [11, 15]. Typically, co-polyesters (5 replicates)

211   were mounted on the top of the transpiration chamber with a 0.6 cm diameter hole, subsequently filled

212   with 300 µL of deionized water, inverted and placed in a desiccator filled with a desiccant. Water transfer

213   across the co-polyesters samples was determined by gravimetric analysis of the transpiration chamber

214   every 8h during 4 days. Water permeance (P) was calculated as the ratio P=F/A.Δc, where F (Flow rate of

215   water) is determined as the slope of water transfer across the samples (in g.s^{-1}), A (in m^2) is the area across

216   which transport has occurred, and Δc (in g.m^{-3}) is the water gradient driving force.

217   The oxygen permeability of co-polyesters was determined in triplicate at 23°C and 0% relative

218   humidity through an isostatic and dynamic method using gas-phase chromatography as previously

219   described [16]. The film samples (4 cm diameter) were placed inside sealed stainless-steel permeability cells.

220   The lower chamber was continuously spread by a 5 mL.min^{-1} flux of permeant gas (O$_2$), and the upper

221   chambers by the same flux of vector gas (helium), thus applying a permanent O$_2$ partial pressure

222   difference. The permeability cells were coupled to a gas chromatograph with thermal conductivity detector

223   (GC-TCD, Agilent 7890A, USA), equipped with an automatic valve to online analyze the evolution with time

224   of O$_2$ gas concentration in the upper chamber. The GC-TCD was equipped with two capillary columns -

225   PoraPlot U (25 m × 0.530 mm id, Agilent) and HP Molesieve (30 m × 0.535 mm id, Agilent) – able to separate

226   O$_2$, CO$_2$ and N$_2$. Data were collected and processed using the ChemStation OpenLab Software (Agilent) and

227   SRA Prochem interface (SRA Instruments). The O$_2$ permeability, P_{O2} (mol.m^{-1}.s^{-1}.Pa^{-1}), of the film samples

228   was calculated as follows:

229    $$P_{O_2} = \frac{J \times e}{A \times \Delta P}$$ (equation1)

230   Where: J (mol.s^{-1}) is the flux of gas that pass through the film, e is the film thickness (m), A is the permeation

231   area (m^2) and ΔP is the O$_2$ pressure differential between the upper and lower chambers of the cell (Pa).
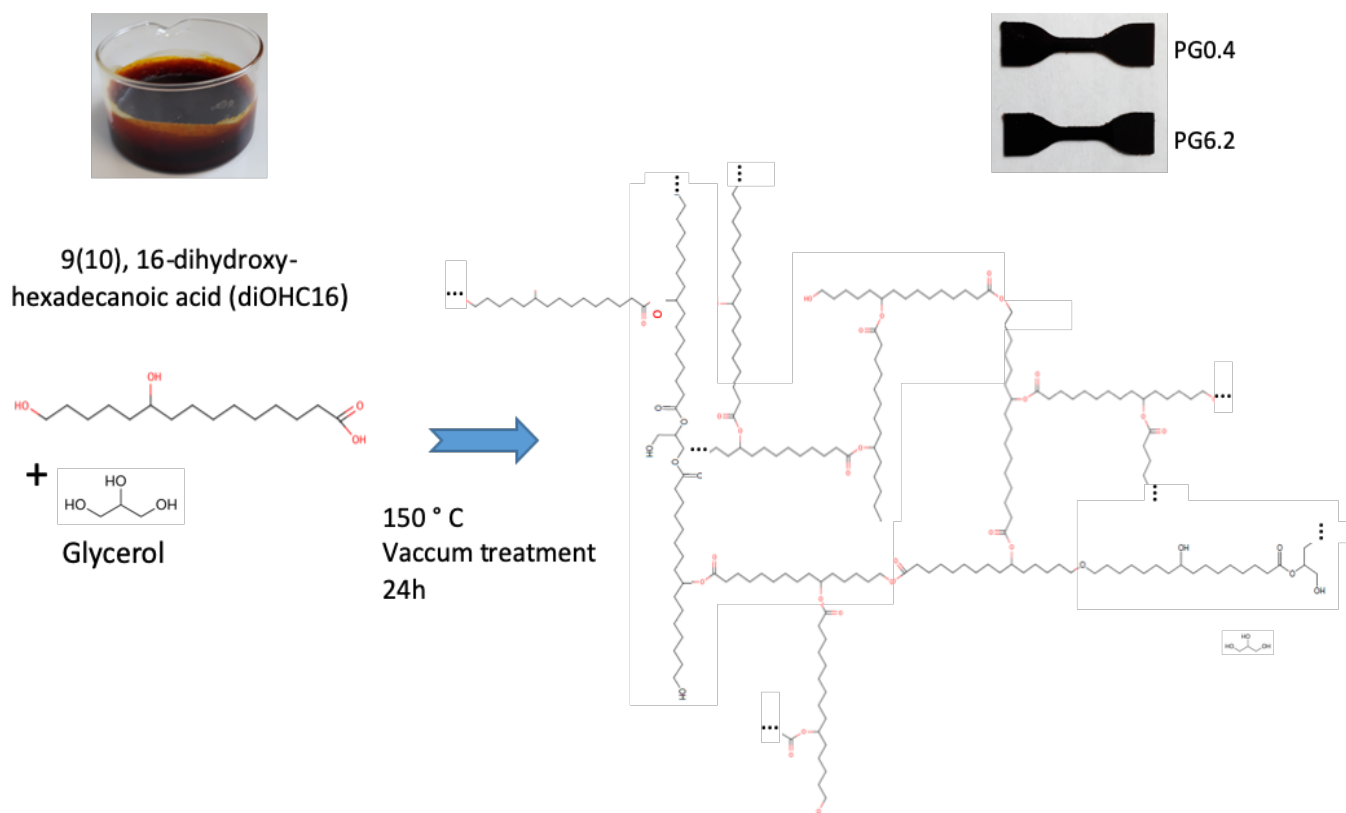
232

233   **Microbiological analyses**

234   *S. aureus* NCTC8325 and *E. coli* TOP 10 cells (10^5 cells·mL^{-1}) in Mueller-Hinton broth (MHB) medium were

235   exposed for 24h to 0.5 cm^2 of polyester films (*ca.* 10 to 20 mg·mL^{-1}) at 37 °C, under orbital agitation (100

236   rpm). Upon incubation, the cellular morphology and the viability of the bacterial cells were visualized by

237   light and fluorescent microscopy, respectively, using a Leica DM6000 B microscope equipped with an iXon

238   EM+ 885 EMCCD camera (Andor Technology®). The fluorescent dye propidium iodide (PI) was used for

239   labelling the dead cells (red fluorescence). Negative controls, i.e., bacteria growing in media devoid of

240   cutin-like co-polyester films, were also carried out. Films from each tested condition were also collected

to scan for the presence of bacterial cells on the film's surface. All assays were done in triplicate. The films were first washed with phosphate buffered saline (PBS) to remove non-adherent bacteria, subsequently fixed with glutaraldehyde 2.5% (v/v) during 10 min. After 10 min, samples were rinsed with distilled water and dehydrated with aqueous solutions with increasing concentration of ethanol (ranging from 70 to 100%). Scanning electron microscopy (SEM) (microscope JEOL JSM-7001F, with an accelerating voltage set to 15 kV) was used to scan the co-polyester film's surfaces. All samples were coated with gold before analysis.

Results and Discussion

Sustainable production of dark black colored insoluble co-polyesters with different ratio of esterified-glycerol

The cutin-like polyesters were manufactured to meet green chemistry and sustainability criteria. Indeed, they were prepared through a catalyst- and solvent-free process using hydroxy-fatty acids and glycerol from renewable resources, i.e., agro-wastes and by-products of the tomato and oilseed processing industries. The hydroxy-fatty acids were extracted following two major biorefinery steps i) fractionation of industrial wastes, i.e., tomato pomaces, into seeds and peels and ii) the processing of peels to recover the hydroxy-fatty acids of the tomato cutin polyester. In both steps, green solvents were used, water and ethanol, which can be recycled to improve the sustainability of the process. The dewaxing step performed in this work, to limit the molecular complexity of this study, could be by-passed, since waxes account for less than 5% (wt.) of tomato cuticles [10]. In contrast with previous studies, the extraction of fatty acids from peels, instead of raw pomaces provided a fatty acid fraction with a higher diOHC16 content (90% instead of 45%)[17]. Interestingly, the alkaline hydrolysis in ethanol at room temperature gave rise to a high fatty acid yield (around 60% wt. of dry peels), instead of around 15% wt. for hot aqueous alkaline hydrolysis [18] thereby strengthening the sustainability of the process. The tomato seeds, a major by-products of pomace biorefinery, can be used for animal feed and human food due to the good nutritional quality of their protein, oil and fiber fractions, or for the production of biogas [19]. Finally, a similar sustainable processing of tomato pomaces was recently developed at the industrial scale for the internal coating of food cans (https://www.tomapaint.com/).

271

Figure 1 – Schematic representation of the solvent- and catalyze-free polycondensation of tomato cutin hydroxyfatty acid and glycerol

272

273

274

275

276

277

278   The cutin-like co-polyesters formed by polycondensation of the diOHC16-rich hydroxy-fatty acid

279   extract and glycerol **(Figure 1)** displayed a dark brown color. All the polyester films were almost insoluble

280   in water, ethanol and chloroform **(Table 1)**. This low solubility of the co-polyesters is therefore ascribed to

281   the formation of cross-linked networks. Minor hydroxy-fatty acids including some dioic acids, as well as

282   phenolic compounds **(supplemental Table 1)** present in the diOHC16 extract, are also insolubilized during

283   polymerization and therefore, are also involved in the formation of the polymer network. In the

284   amorphous polymers produced from whole tomato pomace, it has been proposed that impurities and their

285 oxidation could lead to the formation of additional acid functions during the polymerization, strengthening

286 the formation of cross-linkages [7]. In our case, similar oxidation processes should occur as evidenced by the

287 darkening that occurs during the polymerization process **(Figure 1)**. Although these minor compounds and-

288 or their oxidation products cannot be ignored, all other things being equal, the main variable of this study

289 was the glycerol content. Accordingly, we can follow the modulating effect of glycerol on the properties of

290 the co-polyesters produced from the fatty acid extract from peels provided from tomato pomaces, in line

291 with a vision of a sustainable cutin-inspired chemistry.

292 　　To fulfill this objective, in the aim to monitor the effect of glycerol addition onto the cutin-*like* co-

293 polyesters properties, materials containing different amounts of esterified glycerol were produced. After

294 the poly-condensation reaction, the added glycerol can be (i) free, i.e., non-esterified, acting as an external

295 plasticizer, or (ii) esterified, constituting a polyester monomer. Determination of free and esterified

296 glycerol contents revealed that more than 95% of the glycerol was esterified (**Table 1**).
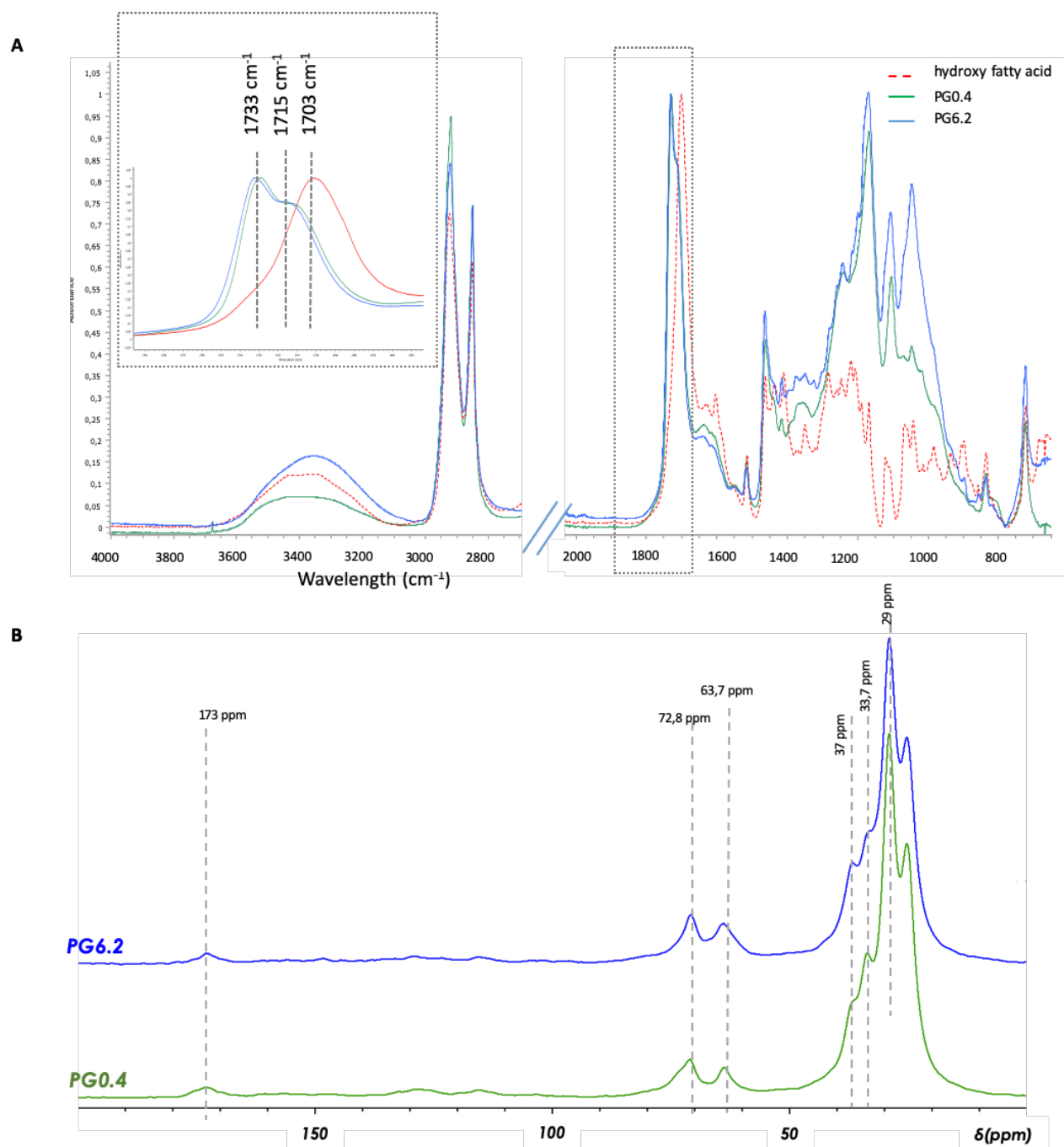
W water, CF chloroform, Et Ethanol

Table 1   Composition, chemical, thermal and mechanical characterization of the cutin-inspired co-polyesters

Sample	Chemical characterisation						DSC					DMTA		Mechanical test		
	glycerol total (%wt)	esterified glycerol (%wt)	free glycerol (% wt)	Insoluble fraction (%) W	Insoluble fraction (%) CF	Insoluble fraction (%) Et	Glass transition temperature (°C)	Melting temperature 1 (°C)	Melting Enthalpy (J/g)	Melting temperature 2 (°C)	Melting Enthalpy (J/g)	Mechanical relaxation temperature (°C)	Storage Modulus at 50°C (MPa)	Breaking stress (MPa)	Strain at break (%)	Young's modulus (Mpa)
PG0.4	0.43 ±0.24	0.38 ± 0.21	0.05 ± 0.04	100	100	98	-8.7	-	-	-	-	8.6	5.867	2.1 ± 0.5	124.0 ± 24.5	2.29 ± 0.05
PG2.3	2.27 ±0.31	2.17 ± 0.32	0.10 ± 0,03	99	100	98	-13.1	-	-	-	-	5.4	5.035	2.0 ± 0.2	155 ± 12.7	1.74 ± 0.06
PG3.9	3.93 ± 0.34	3.75 ± 0.31	0.18 ± 0,05	99	99	94	-15.7	-	-	39.7	0.07	3.2	4.058	1.7 ± 0.2	180.7 ± 10.3	1.26 ± 0.2
PG4.8	4.80 ± 0.82	4.57 ± 0.80	0.23 ± 0.15	99	97	95	-17.0	17.9	0.32	41.6	2.60	1.9	1.408	1.4 ± 0.1	178.4 ± 8.6	1.11 ± 0.03
PG5.2	5.20 ± 0.31	4.87 ± 0.5	0.32 ± 0.2	99	94	91	-20.4	16.8	2.04	41.2	7.96	0.9	1.521	1.3 ± 0.1	197.3 ± 21.1	1.10 ± 0.01
PG6.2	6.18 ± 0.39	5.89 ± 0.45	0.29 ± 0.1	100	88	80	-18.5	18.3	0.59	41,6	9.05	0.2	1.589	1.5 ± 0.1	217.6 ± 14.2	1.19 ± 0.08

A gradual increase of the glycerol content induces a decrease in the branching of the co-polyester films

The co-polyesters containing the lowest (PG0.4) and the highest (PG6.2) levels of esterified glycerol were characterized by ATR- FTIR and ^{13}C NMR (**Figure 2**). ATR-FTIR clearly indicated the formation of esters bonds in these co-polyesters. Indeed, we observed the characteristic shift of the carbonyl band from 1705 cm^{-1}, assigned to the carboxylic acid, to the 1733 cm^{-1} band assigned to the esterified carbonyl[20]. In addition, the 1715 cm^{-1} band assigned to the ester bond involved in hydrogen bonding were also evidenced, as previously observed in tomato cutin [10]. In our present co-polyesters, the hydrogen bonds could involve the free hydroxyl groups either from the hydroxy-fatty acids and/or from the esterified glycerol. Besides, the 1171 cm^{-1} band assigned to the stretching vibration of the C-O-C ester bond was observed in all co-polyesters. Likewise, the ^{13}C C-MAS (**Figure 2B**) data confirmed the formation of esters, evidenced by a single broad peak at 173 ppm and by the peak at 64 ppm, which is assigned to primary esters [17]. In addition, no significant free fatty acid signals were evidenced at 178 ppm (-COOH) and at 35 ppm (-CH$_2$-COOH). Finally, the comparison of the surface ratio of the 33.7 ppm and 37 ppm peaks, assigned to aliphatic carbons (-CH$_2$-CHOR-CH$_2$-) and (CH$_2$-CHOH-CH$_2$) respectively [21], indicated a decrease (40%) in the esterification of the secondary hydroxyls of diOHC16 associated with the increase in the glycerol content.

A . ATR-FTIR spectra of hydroxy-fatty acid (diOHC16) extracted from tomato cutin and the corresponding polymers with high (PG6.2) or low (PG0.4) glycerol. In inset, the magnification of the CO streching bands at 1733 cm^{-1} and 1715 cm^{-1} are assigned respectively to ester group, and ester bond interacting by hydrogen bond whereas the band at 1703 cm^{-1} is assigned to carboxylic group.

B. Solid State ^{13}C CP-MAS NMR spectra of the polymers

Figure 2- ATR-FTIR and NMR spectra of the cutin-like polyesters films

315   The reticulation of the co-polyesters was further monitored by the chemical labelling of the free OH

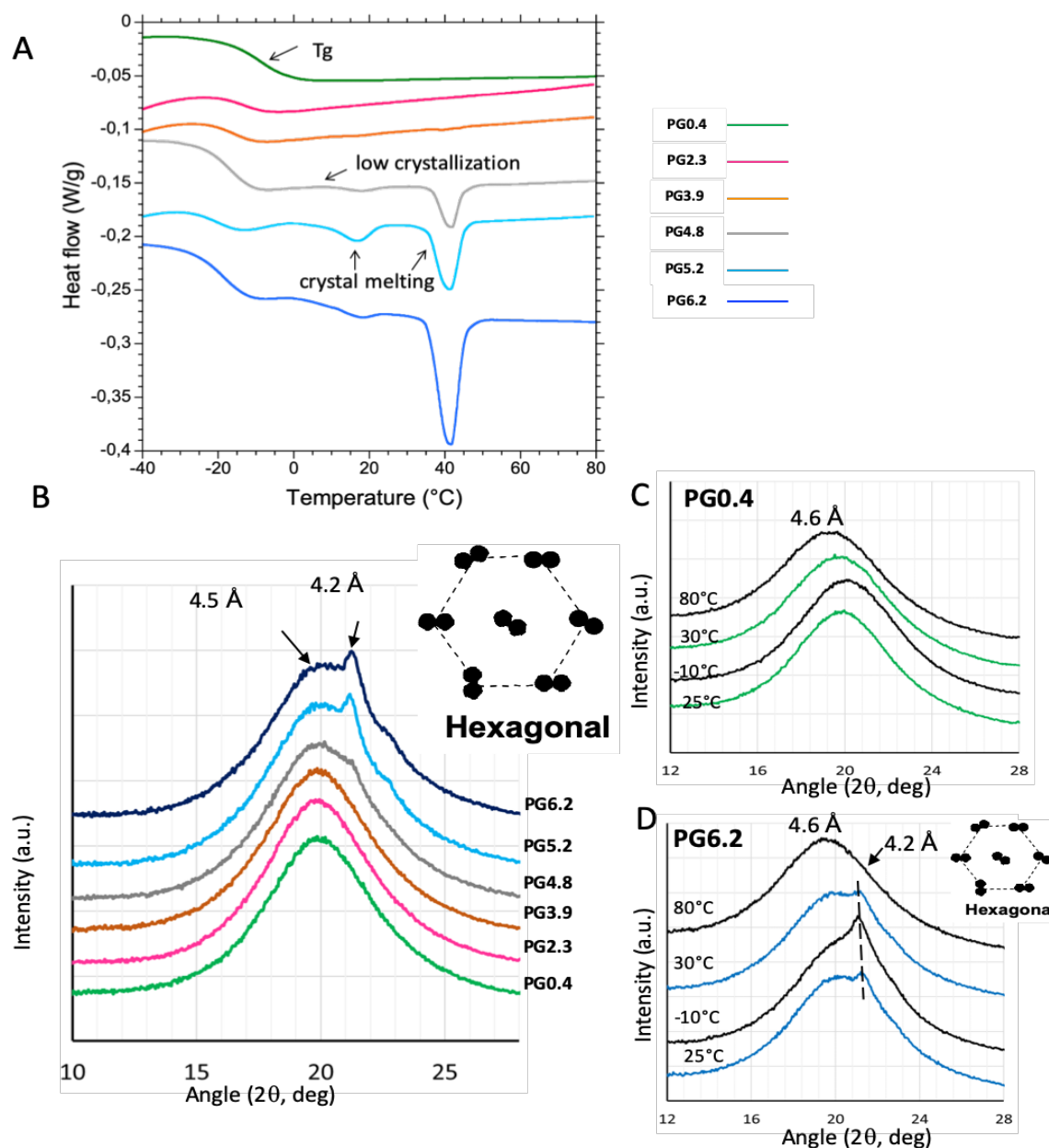316   groups by benzyl ether within the diOHC16-derived polyesters [11] (**Figure 3**).

317

Figure 3. Relative proportion of free OH groups at the ω- and mid-chain position of the the diOHC16 in the co-polyester films.
Values are means of at least three replicates bars are standard deviations

318

319   According to the chemical structure of the diOHC16, both, linear and branched ester bonds, can be

320   formed in the co-polyesters. After complete depolymerization, the release of diOHC16 containing labeled

321   OH groups either in ω-position or in midchain-position was compared in the different co-polyesters. In

322   PG0.4, the ratio of labeled mid-chain OH/ω-OH labeled in diOHC16 was around 9, which indicates that the

323   primary OH groups in the $\omega-$position were preferentially esterified compared to the OH groups in the

324   midchain position. This result agrees with the NMR data (**Figure 2B**) and the previous studies of

325   polycondensation of polyhydroxylated fatty acids [21]. A similar ratio was previously reported for tomato

326   fruit cutin [11]. Furthermore, taking PG0.4 as a reference, the gradual introduction of glycerol in the co-

327   polyesters resulted in a gradual increase (up to 3.5-fold) in the labeled OH groups, in particular in the

328   midchain position. These results indicate that the introduction of glycerol in the co-polyesters induced a

329   gradual decrease in the esterification of midchain hydroxyl groups involved in ester bonds and an increase

330   in the linear polymerization scheme within the co-polyesters.

Glycerol content modulate the elastomer properties of the co-polyesters

The thermal properties of all the produced co-polyesters were investigated by DSC on heating from -50°C to 80°C at 3°C.min^{-1}. Characteristic thermograms are superimposed on the **Figure 4A**.

Figure 4. DSC and XRD analyses of the different cutin-like diOHC16-glycerol co-polyester films

A. DSC thermogram of the different co-polyesters containing increasing level of glycerol from 0.4 % wt (for PG0.4) to 6.2% wt (for PG6.2). **B**, XRD patterns of the different co-polyesters recorded at 25°C., XRD patterns recorded for PG0.4 (**C**) and PG6.2 (**D**) at different temperatures.

336   We checked that the cooling step at -50°C did not modify the crystallinity of the samples. The

337   thermograms of the co-polyesters exhibited various events as a function of the composition, i.e., the

338   amount of esterified glycerol in the samples. From -10°C to -20°C, the baseline fall was attributed to the

339   glass transition characterizing the amorphous phase of the co-polyesters. The glass transition

340   temperatures (Tg), determined at the midpoint of the baseline fall, were determined for each co-polyester

341   (**Table 1**). The Tg value recorded for the PG0.4 sample containing only traces of glycerol is -8.7°C, similar

342   to that measured on polyester catalyst- produced (-7°C) from hydroxy-fatty acids extracted from green

343   tomato cutin [21]. Interestingly, the Tg significantly decreased from -8.7 to -20.4°C with the gradual

344   introduction of glycerol (up to 6.2% wt.) within the co-polyesters, suggesting that the mobility of the co-

345   polyester chains increased giving rise to a more relaxed structure. This result is consistent with the

346   observed reticulation pattern of the co-polyesters (**Figure 3**).

347   For the co-polyesters containing glycerol amounts lower than 4% wt. (PG0.4, PG2.3, PG3.9), the

348   DSC thermograms recorded on heating did not exhibit thermal events above 0°C (**Figure 4A**). However, for

349   the co-polyesters containing higher amounts of glycerol (PG4.8, PG5.2 and PG6.2), endothermic events

350   were recorded and related to the gradual incorporation of glycerol in the materials. Indeed, for these co-

351   polyesters two successive endothermic peaks were recorded around 17°C and 40°C. These endotherms

352   may correspond to structural reorganizations, and/or changes in the physical state of molecules in the co-

353   polyesters. The first peak (17°C), seems to be preceded by an exothermic peak, probably due to a low

354   crystallization event (**Figure 4A**), and exhibits a low enthalpy that could not be clearly related with glycerol

355   content (Table 1). The second endothermic peak (40°C) exhibits a higher enthalpy which increases with the

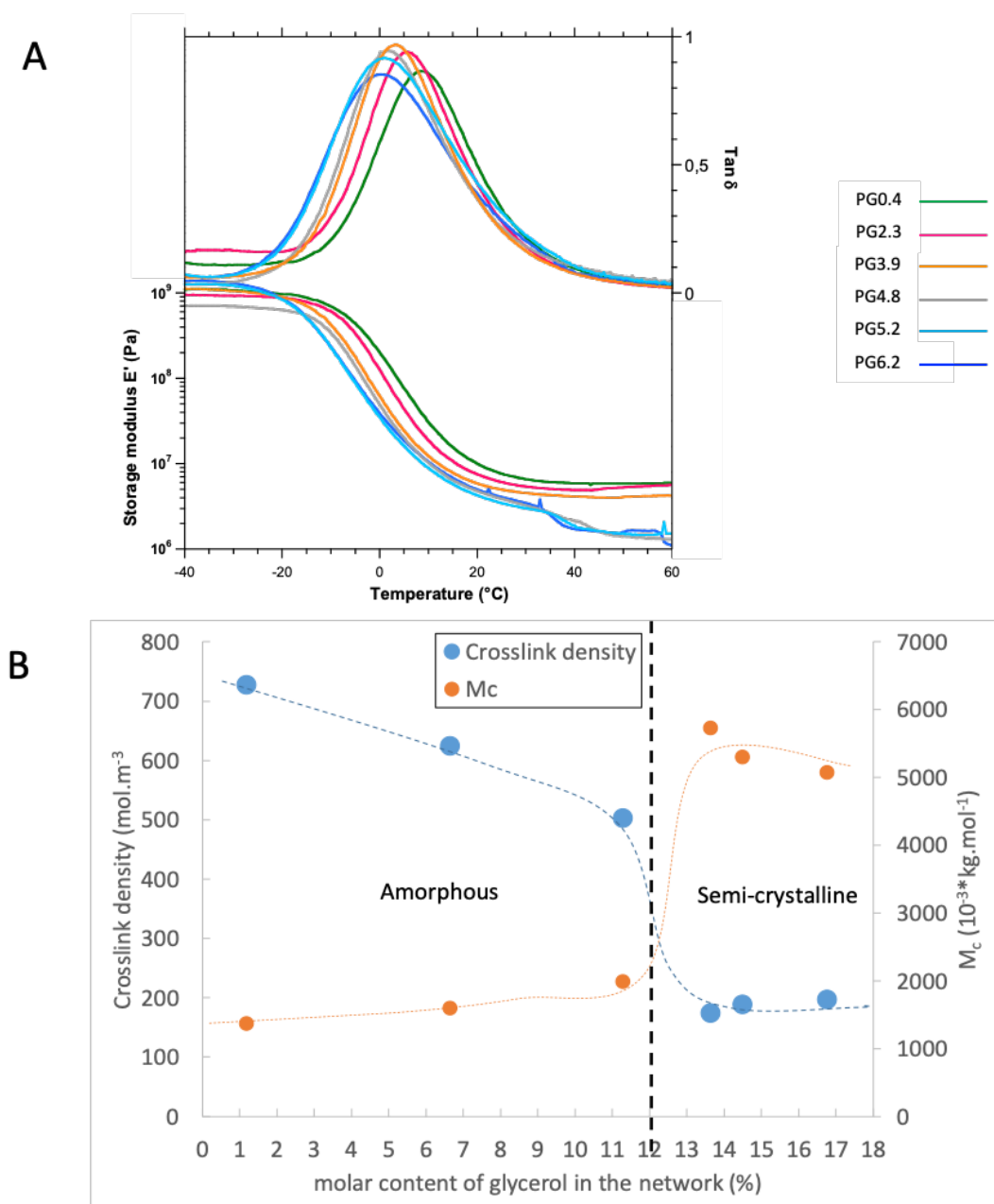356   level of glycerol content (**Table 1**).

357   The X-ray diffraction experiments performed at 25°C showed at wide angles a bump centered at

358   2θ=19° (d=4.5 Å), corresponding to the amorphous state of the co-polyesters (**Figure 4B**). In the co-

359   polyesters containing at least 5 % wt. of glycerol (PG5.2, PG6.2), a peak at 2θ=21.2° was recorded (**Figure

360   4B**). This peak corresponds to a repeat distance of 4.2 Å between the acyl chains that is characteristic of

361   an hexagonal packing of acyl chains. This single peak constitutes the XRD signature of the formation of a

362   crystalline organization of the linear esterified acyl chains within the co-polyesters containing at least 5%

363   wt. glycerol. This XRD peak was superimposed to the bump centered at 4.5 Å (**Figure 4B**), that corresponds

364   to the coexistence of crystalline and amorphous states within the co-polyesters. The presence of glycerol

365   in the samples, and the esterification occurring between the hydroxyl groups of glycerol (mainly in *sn-1*

366   and *sn-3* positions) and the carboxyl groups of the fatty acids induced a linear organization of the chains

367   or the formation of shorter chains. This spatial proximity between the linear and shorter co-polyester

368   chains may favor short-distance hydrophobic interactions between the acyl chains and result in a

369   crystalline organization with a hexagonal packing below the melting temperature of the fatty acids. In

370   absence of glycerol, the reticulation involves the hydroxyl groups both in midchain hydroxyl and ω-

371   positions. This prevents short-distance hydrophobic interactions between the linear chains formed by

372   primary esterification, hence avoiding the formation of a crystalline organization in the co-polyesters.

373   The thermotropic phase behavior of the co-polyesters formed with very low (PG0.4) or high (PG6.2)

374   amount of glycerol, were investigated by XRD at various temperatures ranging from -10°C to 80°C that

375   have been selected according to the DSC results (**Figure 4A**). In presence of very low glycerol content

376   (**Figure 4C**), the amorphous state of the polyester was characterized by a bump of RX diffusion, centered

377   in a mean value that was affected by the temperature. Increasing the temperature induced a shift toward

378   lower angle values corresponding to higher distances between the acyl chains associated with an increase

379   in the molecular mobility. In the presence of 6 % wt. of glycerol (**Figure 4D**), the XRD experiments were

380   conducted at 25°C, then the samples were cooled to -10°C, heated to 30°C (i.e., above the first endotherm)

381   and then finally to 80°C (i.e., above the second endotherm). The single peak at $2\theta=21.2°$ (4.2 Å) was

382   recorded at 25°C, confirming the results previously obtained. Decreasing the temperature to -10°C

383   increased the intensity of the XRD peak at $2\theta=21.2°$ related to a hexagonal phase and was interpreted as

384   an increase in the amount of the crystalline phase formed in the co-polyesters. On heating at 30°C, the

385   intensity of the XRD decreased. Increasing the temperature at 80°C, i.e., above the second endotherm

386   recorded by DSC and then above the melting point of the crystalline structures, induced the disappearance

387   of the XRD peak at $2\theta=21.2°$and to the recording of an XRD bump centered at 4.6 Å characteristic of acyl

388   chains in a melted state. These XRD experiments evidenced the temperature-dependent behavior of the

389   co-polyester, with presence of various amounts of hexagonal phase as a function of temperature.

390   The two endotherms revealed successively by DSC correspond to independent packing events of

391   the molecules both organized in an hexagonal form as revealed by XRD. The different melting

392   temperatures may correspond to packing of molecules with various compositions, *e.g.* chain length.

393   The thermo-mechanical behavior of all co-polyesters were analyzed by DMTA. **Figure 5A** shows the

394   plot of the storage modulus (E') and the loss factor tan δ of the co-polyesters.

Figure 5 – DMA analysis of the cutin-like diOHC16-glycerol co-polyesters

A – Plot of the storage modulus (E') and the loss factor tan δ of the co-polyesters with different level of esterified glycerol content.
B- Evolution of the crosslink density and the average mass between crosslinks as a function of the molar content of glycerol in the network. Dashed lines are just guides for the eyes.

395

396   For all samples, the large peak of tan δ corresponds to the main mechanical relaxation α which is

397   associated to the calorimetric glass transition of the elastomer (transition from glassy to rubbery state).

398   The relaxation temperature from the glassy to the rubbery state ($T\alpha$), determined at the maximum of the

399   tan δ curve, decreases from 8.6°C to 0.2°C when glycerol content increases (**Table 1**). In agreement with

400   the Tg values obtained by DSC analyses (**Table 1**) such depressor effect of glycerol on $T\alpha$ further

401   strengthens the impact of the glycerol on the properties of the cutin-like co-polyesters.

402   A second event appears on storage modulus which slightly fall in the temperature range 30-40°C

403   for the composition containing more than 4% (wt.) of glycerol (PG4.8, PG5.2, PG6.2) (**Figure 5A**). This

404   transition is attributed to the melting of the crystalline phase according to DSC and XRD results (**Figure 4**).

405   Finally, the plateau of storage modulus is reached at about 50°C with a value which decreases from 5.867

406   MPa to 1.589 MPa when glycerol content increases from 0.4 to 6% wt. (**Table 1**).

407

408   Since these values are typical of rubber elasticity, the Flory theory [22] may be used to relate them to

409   the structure of the networks[23]. Accordingly, the crosslink density v (mole.m^{-3}) is given by:

410 $$v = \frac{E}{3RT} \qquad \text{(equation 2)}$$

411   Where: R is the gas constant 8.32 J.mol^{-1}.K^{-1}, T is the temperature in Kelvin and E the elastic modulus at

412   small deformation.

413   Therefore, the average molecular mass Mc (kg.mol^{-1}) between crosslinks is:

414 $$M_c = \frac{3RT\rho}{E} \qquad \text{(equation 3)}$$

415   Where: ρ is the density of the material in Kg.m^{-3}. In the present case, E corresponds to the plateau storage

416   modulus measured in DMTA at 50°C (T = 323 K). The density of the co-polyesters at this temperature could

417   not be measured. As a first approximation, we considered a constant density ρ= 1000 kg.m^3 for the

418   calculations reported in **Table 2 and Figure 5B.**

	n	$M_{c\ (g/mol)}$	M_c/M_0	Esterified molar glycerol content *
	(mol.m^{-3})	(10^{-3} kg.mol^{-1})	-	mol %
PG 0.4	728	1374	5.1	1.2
PG 2.3	625	1601	5.9	6.64
PG 3.9	503	1987	7.4	11.3
PG 4.8	175	5726	21.2	13.6
PG 5.2	189	5301	19.6	14.5
PG 6.2	197	5074	18.8	16.8

* the molar content of glycerol in the networks given by

$$esterified\ Glycerol\ (mol\%) = \frac{\frac{esterified\ glycerol\ w\%}{M_{glycerol}}}{\frac{esterified\ glycerol\ w\%}{M_{glycerol}} + \frac{(100 - free\ glycerol\ w\% - esterified\ glycerol\ w\%)}{M_{diOHC16}}}$$

Table 2 : Macromolecular structure of the network predicted by the Flory theory

419

420

421 The elastomers PG0.4, PG2.3 and PG3.9 show the largest crosslink density values in the range of 500- to

422 730 mol.m^{-3} associated to small values of M_c in the 1300-2000 g.mol^{-1} range. Concurrently, much lower

423 values of ν (175 to 200 mol.m^{-3}) are obtained for samples PG4.8, PG5.2 and PG6.2, with higher values of

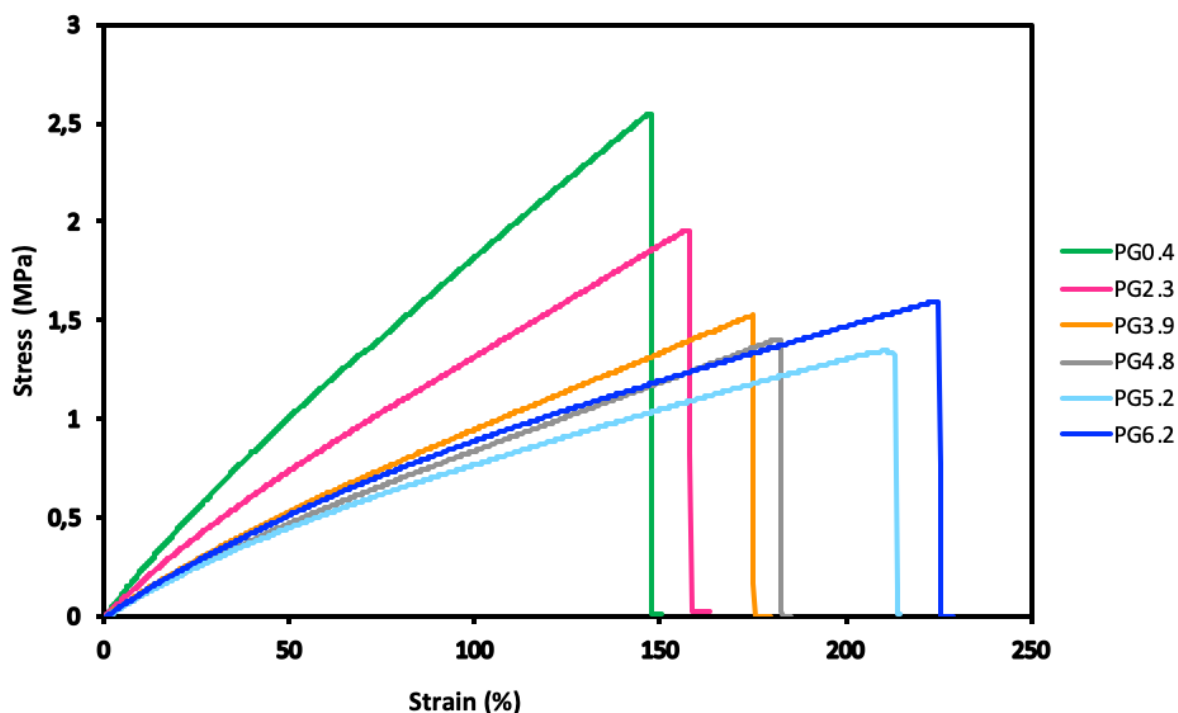424 M_c in the 5000-5700 g.mol^{-1} range.

425 In a first approximation, the number of polymerized diOHC16 repeating units between crosslinks

426 can be estimated by dividing these values of M_c by a repeating unit mass M_0= 270 g.mol^{-1} (this value

427 assumes that elastically active chains consist essentially of polymerized diOHC16 monomer units in which

428 only 1 acid and 1 hydroxyl group have reacted.)

429 The values of the ratio M_c/M_0 calculated in **Table 2** suggest that for samples PG0.4, PG2.3 and PG3.9

430 the number of polymerized diOHC16 repeating units should range from 5 to 7, while 19 to 21 repeating

431 units are predicted for samples PG4.8, PG5.2 and PG6.2. For these latter, a few glycerol units are probably

432 also present in the elastically active chains. Anyhow, such a loosening of the network induced by the

433 gradual introduction of the glycerol is in full accordance with the increase in the labelling of free OH groups

434 within the co-polyesters (**Figure 3**).

435 Besides, the plot of ν and M_c as a function of this molar content of glycerol chemically bound to the

436 network is shown on Figure 5B. A sharp transition from dense amorphous networks (PG0.4, PG2.3 and

437 PG3.9) to loose semi-crystalline networks (PG4.8, PG5.2 and PG6.2) seems to take place around a threshold

438 value of 12 mol% of glycerol.

439   The development of a crystallinity for higher glycerol contents may be ascribed to the flexibility of

440   the long chain segments between two crosslinks which become able to fold into crystallites, while at lower

441   glycerol content the shorter chains remain amorphous.

442   According to the different chemical structures highlighted by the structural and thermal

443   characterization of the different co-polyesters, we further checked their tensile mechanical properties. The

444   determined tensile strength, strain at break and Young Modulus are reported on **Table1**, and the

445   characteristic curve are superimposed on the **Figure 6**.

446

**Figure 6- Typical Stress-strain curves of the cutin-like diOHC16-glycerol
co-polyester films from 0.4 % wt. for PG0.4 to 6.2% wt. for PG6.2**

447

448

449   All co-polyesters, either with low or high content of glycerol, show a quasi linear and reversible

450   stress-strain behavior that is characteristic of polyesters exhibiting rubber elasticity comparable to

451   synthetic elastomers. The mechanical properties of the PG0.4, were comparable to those previously
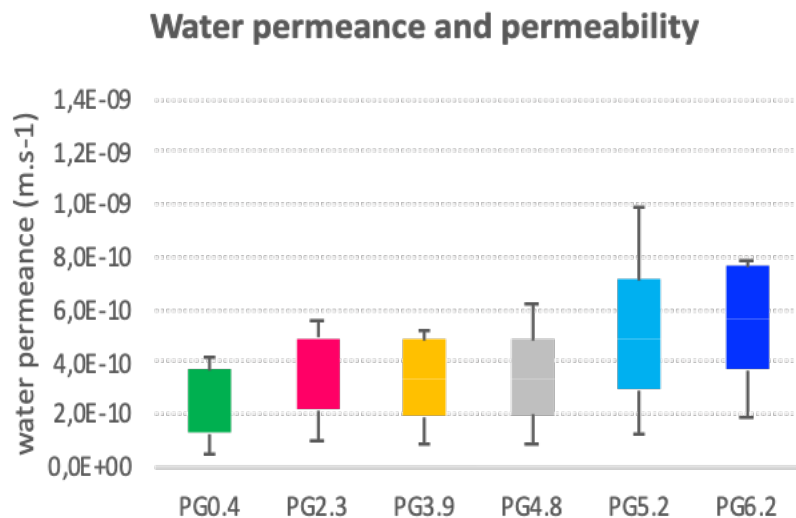
452 described with other polyhydroxylated fatty acids[21, 24]. Moreover, our present data show that the

453 mechanical properties were strongly modified by the gradual introduction of glycerol in the co-polyesters

454 which resulted in a decrease in the Young modulus (from 2.29 to 1. 19 MPa), as well as in the stress at

455 break (from 2.1 to 1.5 MPa). Surprisingly, higher glycerol of 6% induces a slight increase of tensile strength

456 simultaneous to the increase of strain at break. It is certainly due to the crystallinity evidenced by

457 calorimetry and XRD measurements (Figure 4).

458 The most striking observation is the increase in strain at break from 124% to 217 % (for PG0.4 and

459 PG6.2 respectively) induced by the esterified glycerol in the co-polyesters **(Table1, Figure 6**). This

460 elongation value is comparable to some synthetic rubber such as ethylene-propylene-diene or polysulfide-

461 butadiene rubbers[25]. This strain at break induced by an higher glycerol/hydroxy-fatty acid ratio fully fits

462 the CUS1 tomato phenotype which is affected in cutin deposition[11]. Importantly, the CUS1 tomato cutin

463 polyester exhibited a fivefold increase in the glycerol ratio (vs hydroxylated fatty acids), which probably

464 account for the increase in its extensibility and the absence of cracks observed on the CUS1 fruits,

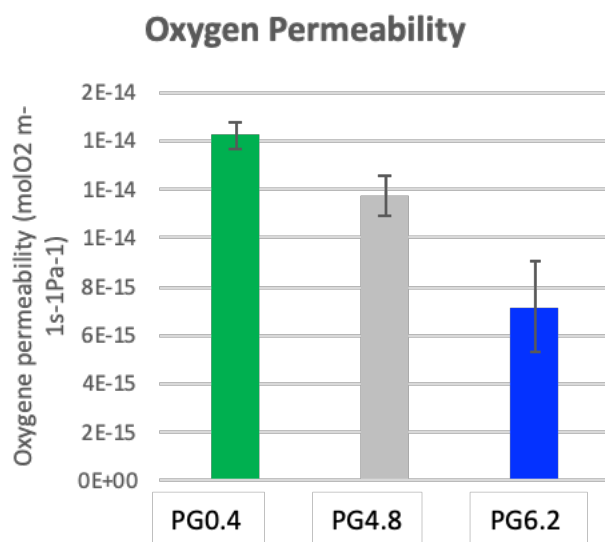465 regardless that their cuticle density shows a threefold reduction [10].

466

467

468 **Glycerol can modify the barrier properties of the co-polyesters and their interaction with bacterial cells**

469 Water permeance and oxygen barrier properties of the co-polyesters were analyzed. All the produced co-

470 polyesters showed low water vapor permeance properties (**Figure 7A**) around 10^{-9} m.s^{-1}, in the same range

471 than the plant cuticle permeance and some synthetic membrane, such as 3µm parafilm or 3µm

472 polyethylene [26]. The introduction of esterified glycerol and the associated modification of the branching of

473 the co-polyesters induced a slight, but statistically not significant increase in the water vapor permeability

474 of the co-polyesters. This result is consistent with our previous data showing that a modification of the

475 polymerization index did not significantly impact the water permeance of tomato cutins (Philippe et al,

476 2016).

477

Figure 7- Barrier properties of the cutin-like co-polyesters
Water permance (A) and Oxygen (B) barrier properties of the cutin-like diOHC16-glycerol co-polyesters containing increasing level of glycerol (0.4 %wt for PG0.4 to 6.2% wt for PG6.2)

478

479

480   The oxygen permeability of the cutin-derived co-polyesters ranged between 0.7 and 1.4 x 10^{-14} mol

481    $m^{-1} s^{-1} Pa^{-1}$ (Figure 7B). These values are in the same order of magnitude of synthetic polymers commonly

482   used for food packaging such as low-density polyethylene (0.1-0.2 x 10^{-14} $mol.m^{-1}.s^{-1}.Pa^{-1}$) [16, 27, 28]. These

483   values are also comparable to polylactic acid (PLA), a bio-based polyester, for which oxygen permeability

484   values ranging between $1x10^{-16}$ and $1x10^{-14}$ mol. $m^{-1}.s^{-1}.Pa^{-1}$ have been reported [29-31]. Other polyesters such

485　as fossil-based polyethylene terephthalate, or microbial synthesized polyhydroxyalkanoates (PHAs) have

486　considerably higher barrier properties with oxygen permeability in the order of 1×10^{-17} mol m^{-1} s^{-1} Pa^{-1} [32,

487　33].

488　　　　Interestingly, increasing the ratio of esterified glycerol in the co-polyesters improved the films

489　oxygen barrier properties by reducing oxygen permeability by half (**Figure 7B**). This is probably associated

490　with the increase of crystallinity, as observed for other elastomers [34] reducing the motion needed for

491　oxygen diffusion.

492　　　　Finally, the antibacterial activity of the co-polyesters containing the lowest and the highest levels

493　of esterified glycerol (PG0.4 and PG6.2) was assessed on *E. coli* and *S. aureus*. After exposure to the co-

494　polyester films, no labelling of dead cells was revealed (**Figure 8A**), which indicates that the co-polyesters

495　were devoid of bactericidal properties regardless of the glycerol content. This result contrasts with the

496　biocide activity that was demonstrated with acyl glycerol esters of hydroxy-fatty acids [35] or with films

497　formed by self-assembly of these esters [36, 37] extracted by an ionic liquid catalyst from suberin, another

498　hydrophobic plant polyesters.

499　　　　Since the co-polyesters are devoid of bactericidal capacity, we further analyzed the films' surface

500　following their incubation with bacteria (**Figure 8 B**). For either co-polyester, the numbers of adherent *E.*

501　*coli* cells were low and comparable. Remarkably over the surface of the PG0.4 co-polyester, *S. aureus*

502　formed a compacted biofilm whereas PG6.2 hinder significantly the adhesion of this bacteria species. This

503　result demonstrates that increased glycerol levels in the cutin inspired co-polyesters leads to significant

504　reducing of bacterial fouling. (**Figure 8 B**). The observed differences between the two bacteria species

505　might be due to the electronegativity of the cells surface that is higher in *E. coli* than *S. aureus*, regardless

506　that their different morphologies and surface roughness (rods and cocci, respectively) may greatly

507　influence their adhesion in the conditions used here. This observation, supported by the structural, thermal

508　and mechanical analyses, suggests that glycerol esterification altered the smoothness of the films' surface

509　as well as their surface charge. One important finding is that by increasing further the glycerol levels in the

510　cutin co-polyesters their anti-biofouling properties can be potentiated.

511

Figure 8. Microscopy imaging of the cutin-like co-polyesters PG0.4 and PG6.2 after incubation with *E. coli* and *S. aureus*.

A. Co-polyesters films activity against *E. coli* and *S. aureus*. Following exposure of bacteria to films pieces their morphology and viability were visualized by phase-contrast and fluorescence microscopy using Texas Red filter (dead cells are reveald by red fluorescence due to propidium iodide labelling), respectively. Controls was conducted without films. The scale bar in all images is 5μm.

B. Cells adherent onto the surface of the cutin co-polyester films were observed by SEM microscopy. No differences were noticed in the numbers of adherent *E. coli* cells in either co-polyester films. Conversely, the number of *S. aureus* adherent cells (ex under arrows) are significantly higher in the PG0.4 co-polyester compared to the PG6.2. The scale bar in all images is shown at the bottom.

512

Conclusions

We report in this work, the sustainable production of glycerol/hydroxy-fatty acid co-polyesters by a catalyst- and solvent-free polycondensation process. Glycerol and hydroxy-fatty acids are biosourced molecules from by-products and wastes produced by the oilseed and tomato processing industries, respectively. The hydroxy-fatty acid fraction used in this work was prepared using an improved process compared to what is done today on an industrial scale. Therefore, the production of these glycerol/hydroxy-fatty acid co-polyesters meets the requirements of green chemistry and sustainability. These co-polyesters are inspired from the cutin polymer of plant cuticles, which is also composed of hydroxy-fatty acids and glycerol. Drawing on our previous studies on tomato fruit cuticle, we gradually increased the glycerol content while remaining in a concentration range observed in most plant cuticles. This biomimetic approach can be seen as a step forward in the production of natural elastomeric networks which is a very active field for instance from natural rubber[23, 38]. The produced co-polyesters displayed good elastomers properties, quite comparable to those of some synthetic rubber polymers. By adjusting the level of esterified glycerol, we induced modifications of the reticulation pattern which was associated to variation in chain mobility and extensibility. Glycerol also induced the loosening of the co-polyester network and the formation of crystalline domains. These modifications were associated to variations in the mechanical and barrier properties of the co-polyesters as well as adhesion of microorganisms.

Actually, these hydroxy-fatty acid/glycerol co-polyesters provide excellent templates to further delineate the relationships between the complex molecular and macromolecular architecture and the functional properties of plant cuticular barriers, while developing green polymer composites adapted to specific applications for food, packaging industry or as antifouling natural product. Furthermore, increasing contents of glycerol led to available free hydroxyl groups for grafting and covalent substitutions for tailored functionalization, opening new routes for high-value applications (e.g., in the medical sector).

542

References

543
544

545   1.   Fich, E. A.; Segerson, N. A.; Rose, J. K., The plant polyester cutin: biosynthesis, structure, and
546   biological roles. *Annu. Rev. Plant Biol.* **2016,** *67*, 207-233.https://doi.org/10.1146/annurev-arplant-
547   043015-111929
548   2.   Nawrath, C., Unraveling the complex network of cuticular structure and function. *Curr. Opin. Plant*
549   *Biol.* **2006,** *9* (3), 281-287.https://doi.org/10.1016/j.pbi.2006.03.001
550   3.   Yeats, T. H.; Rose, J. K., The formation and function of plant cuticles. *Plant Physiol.* **2013,** *163* (1),
551   5-20.https://doi.org/10.1104/pp.113.222737
552   4.   Fameau, A.-L.; Gaillard, C.; Marion, D.; Bakan, B., Interfacial properties of functionalized
553   assemblies of hydroxy-fatty acid salts isolated from fruit tomato peels. *Green Chem.* **2013,** *15* (2), 341-
554   346.https://dori.org/10.1039/C2GC36677K
555   5.   Heredia-Guerrero, J. A.; Heredia, A.; Dominguez, E.; Cingolani, R.; Bayer, I. S.; Athanassiou,
556   A.; Benitez, J. J., Cutin from agro-waste as a raw material for the production of bioplastics. *J. Exp. Bot.*
557   **2017,** *68* (19), 5401-5410.https://doi.org/10.1093/jxb/erx272
558   6.   Fritsch, C.; Staebler, A.; Happel, A.; Cubero Márquez, M. A.; Aguiló-Aguayo, I.; Abadias, M.;
559   Gallur, M.; Cigognini, I. M.; Montanari, A.; López, M. J.; Suárez-Estrella, F.; Brunton, N.; Luengo, E.;
560   Sisti, L.; Ferri, M.; Belotti, G., Processing, valorization and application of bio-waste derived compounds
561   from potato, tomato, olive and cereals: A Review. **2017,** *9* (8), 1492.https://doi.org/doi:10.3390/su9081492
562   7.   Benítez, J. J.; Castillo, P. M.; Del Río, J. C.; León-Camacho, M.; Domínguez, E.; Heredia, A.;
563   Guzmán-Puyol, S.; Athanassiou, A.; Heredia-Guerrero, J. A., Valorization of tomato processing by-
564   products: fatty acid extraction and production of bio-based materials. *Materials (Basel)* **2018,** *11*
565   (11).https://doi.org/10.3390/ma11112211
566   8.   Quispe, C. A. G.; Coronado, C. J. R.; Carvalho Jr, J. A., Glycerol: production, consumption,
567   prices, characterization and new trends in combustion. *Renew. Sust. Energ. Rev.* **2013,** *27*, 475-
568   493.https://doi.org/10.1016/j.rser.2013.06.017
569   9.   Graça, J.; Schreiber, L.; Rodrigues, J.; Pereira, H., Glycerol and glyceryl esters of omega-
570   hydroxyacids in cutins. *Phytochemistry* **2002,** *61* (2), 205-215.https://doi.org/10.1016/s0031-
571   9422(02)00212-1
572   10.   Girard, A. L.; Mounet, F.; Lemaire-Chamley, M.; Gaillard, C.; Elmorjani, K.; Vivancos, J.;
573   Runavot, J. L.; Quemener, B.; Petit, J.; Germain, V.; Rothan, C.; Marion, D.; Bakan, B., Tomato
574   GDSL1 is required for cutin deposition in the fruit cuticle. *Plant Cell* **2012,** *24* (7), 3119-
575   34.https://doi.org/10.1105/tpc.112.101055
576   11.   Philippe, G.; Gaillard, C.; Petit, J.; Geneix, N.; Dalgalarrondo, M.; Bres, C.; Mauxion, J. P.;
577   Franke, R.; Rothan, C.; Schreiber, L.; Marion, D.; Bakan, B., Ester cross-link profiling of the cutin
578   polymer of Wild-Type and cutin synthase tomato mutants highlights different mechanisms of
579   polymerization. *Plant Physiol.* **2016,** *170* (2), 807-20.https://doi.org/10.1104/pp.15.01620
580   12.   Barker, J. C., Russeting (cuticle cracking) in glasshouse tomatoes in relation to fruit growth. *J.*
581   *Hortic. Sci.* **1988,** *63* (3), 459-463.https://doi.org/10.1080/14620316.1988.11515879
582   13.   Philippe, G.; Geneix, N.; Petit, J.; Guillon, F.; Sandt, C.; Rothan, C.; Lahaye, M.; Marion, D.;
583   Bakan, B., Assembly of tomato fruit cuticles: a cross-talk between the cutin polyester and cell wall
584   polysaccharides. *New Phytol.* **2020,** *226* (3), 809-822.https://doi.org/10.1111/nph.16402
585   14.   Shen, Y.; Xu, Z., An improved GC-MS method in determining glycerol in different types of
586   biological samples. *J. Chromatogr. B Analyt. Technol. Biomed. Life Sci.* **2013,** *930*, 36-
587   40.https://doi.org/10.1016/j.jchromb.2013.04.034
588   15.   Schreiber L; J, S. n., Water Permeability. In *Water and solute permeability of plant cuticles*,
589   Springer Berlin Heidelberg: Berlin, Heidelberg, 2009; pp 61-123.

590   16.   Motedayen, A. A.; Rezaeigolestani, M.; Guillaume, C.; Guillard, V.; Gontard, N., Gas barrier
591   enhancement of uncharged apolar polymeric films by self-assembling stratified nano-composite films.
592   *RSC Advances* **2019,** *9* (19), 10938-10947.https://doi.org/10.1039/C9RA01109A
593   17.   Tedeschi, G.; Benitez, J. J.; Ceseracciu, L.; Dastmalchi, K.; Itin, B.; Stark, R. E.; Heredia, A.;
594   Athanassiou, A.; Heredia-Guerrero, J. A., Sustainable fabrication of plant cuticle-like packaging films from
595   tomato pomace agro-waste, beeswax, and alginate. *ACS Sustainable Chem. Eng.* **2018,** *6* (11), 14955-
596   14966.https://doi.org/10.1021/acssuschemeng.8b03450
597   18.   Cogognigni, I.; Montanari, A.; de la Torre Carreras, R.; Cardoso Bernet Montserrat, G. Extraction
598   method of a polyester polymer or cutin from the wasted tomato peels and polyester polimer so extracted
599   WO/2015/028299, 2014.
600   19.   Lu, Z.; Wang, J.; Gao, R.; Ye, F.; Zhao, G., Sustainable valorisation of tomato pomace: A
601   comprehensive review. *Trends Food Sci. Technol.* **2019,** *86*, 172-
602   187.https://doi.org/10.1016/j.tifs.2019.02.020
603   20.   Heredia-Guerrero, J. A.; Benítez, J. J.; Domínguez, E.; Bayer, I. S.; Cingolani, R.; Athanassiou,
604   A.; Heredia, A., Infrared and Raman spectroscopic features of plant cuticles: a review. *Front. Plant Sci.*
605   **2014,** *5*, 305.https://doi.org/10.3389/fpls.2014.00305
606   21.   Benitez, J. J.; Heredia-Guerrero, J. A.; Guzman-Puyol, S.; Barthel, M. J.; Dominguez, E.;
607   Heredia, A., Polyhydroxyester films obtained by non-catalyzed melt-polycondensation of natural occurring
608   fatty polyhydroxyacids. *Front. Mat.* **2015,** *2*, 10.https://doi.org/10.3389/fmats.2015.00059
609   22.   Flory, J. P., Elasticity of rubber. In *Principles of Polymer Chemistry*,   Ithaca, N.Y. : Cornell
610   University Press ed.; 1953; Vol. 11.
611   23.   Tran, T.-N.; Guyomard-Lack, A.; Cerclier, C.; Humbert, B.; Colomines, G.; Pilard, J.-F.;
612   Deterre, R.; Bideau, J.-L.; Leroy, E., Natural rubber-based ionogels. **2018,** *6* (3), 251--
613   258.https://doi.org/doi:10.7569/JRM.2017.634174
614   24.   Benítez, J. J.; Heredia-Guerrero, J. A.; Guzmán-Puyol, S.; Domínguez, E.; Heredia, A., Long-
615   chain polyhydroxyesters from natural occurring aleuritic acid as potential material for food packaging. *Soft*
616   *Materials* **2015,** *13* (1), 5-11.https://doi.org/10.1080/1539445X.2014.993476
617   25.   Shanks, R. A.; Kong, I., General purpose elastomers: structure, chemistry, physics and
618   performance. In *Advances in Elastomers I: Blends and Interpenetrating Networks*, Visakh, P. M.;
619   Thomas, S.; Chandra, A. K.; Mathew, A. P., Eds. Springer Berlin Heidelberg: Berlin, Heidelberg, 2013;
620   pp 11-45.
621   26.   Valeska Zeisler-Diehl, V.; Migdal, B.; Schreiber, L., Quantitative characterization of cuticular
622   barrier properties: methods, requirements, and problems. *J. Exp. Bot.* **2017,** *68* (19), 5281-
623   5291.https://doi.org/10.1093/jxb/erx282
624   27.   Durmuş, A.; Woo, M.; Kaşgöz, A.; Macosko, C. W.; Tsapatsis, M., Intercalated linear low density
625   polyethylene (LLDPE)/clay nanocomposites prepared with oxidized polyethylene as a new type
626   compatibilizer: Structural, mechanical and barrier properties. *Eur. Polym. J.* **2007,** *43* (9), 3737-
627   3749.https://doi.org/10.1016/j.eurpolymj.2007.06.019
628   28.   Matar, C.; Gaucel, S.; Gontard, N.; Guilbert, S.; Guillard, V., Predicting shelf life gain of fresh
629   strawberries 'Charlotte cv' in modified atmosphere packaging. *Postharvest Biol. Technol.* **2018,** *142*, 28-
630   38.https://doi.org/10.1016/j.postharvbio.2018.03.002
631   29.   Lehermeier, H. J.; Dorgan, J. R.; Way, J. D., Gas permeation properties of poly(lactic acid). *J.*
632   *Membr. Sci.* **2001,** *190* (2), 243-251.https://doi.org/10.1016/S0376-7388(01)00446-X
633   30.   Mahmoodi, A.; Ghodrati, S.; Khorasani, M., High-strength, low-permeable, and light-protective
634   nanocomposite films based on a hybrid nanopigment and biodegradable PLA for food packaging
635   applications. *ACS Omega* **2019,** *4* (12), 14947-14954.https://doi.org/10.1021/acsomega.9b01731
636   31.   Palai, B.; Biswal, M.; Mohanty, S.; Nayak, S. K., In situ reactive compatibilization of polylactic
637   acid (PLA) and thermoplastic starch (TPS) blends; synthesis and evaluation of extrusion blown films
638   thereof. *Industrial Crops and Products* **2019,** *141*, 111748.https://doi.org/10.1016/j.indcrop.2019.111748
639   32.   Ambrosio-Martin, J.; Fabra, M. J.; López-Rubio, A.; Gorrasi, G.; Sorrentino, A.; Lagaron, J. M.,
640   Assessment of ball milling as a compounding technique to develop nanocomposites of poly(3-

hydroxybutyrate-co-3-hydroxyvalerate) and bacterial cellulose nanowhiskers. *J. Polym. Environ.* **2016,** *24* (3), 241-254.https://doi.org/10.1007/s10924-016-0767-6

33.   Crétois, R.; Follain, N.; Dargent, E.; Soulestin, J.; Bourbigot, S.; Marais, S.; Lebrun, L., Microstructure and barrier properties of PHBV/organoclays bionanocomposites. *J. Membr. Sci.* **2014,** *467*, 56-66.https://doi.org/10.1016/j.memsci.2014.05.015

34.   Wang, Y.; Gupta, M.; Schiraldi, D. A., Oxygen permeability in thermoplastic polyurethanes. **2012,** *50* (10), 681-693.https://doi.org/10.1002/polb.23053

35.   Correia, V. G.; Bento, A.; Pais, J.; Rodrigues, R.; Haliński, Ł. P.; Frydrych, M.; Greenhalgh, A.; Stepnowski, P.; Vollrath, F.; King, A. W. T.; Silva Pereira, C., The molecular structure and multifunctionality of the cryptic plant polymer suberin. *Materials Today Bio* **2020,** *5*, 100039.https://doi.org/10.1016/j.mtbio.2019.100039

36.   Ferreira, R.; Garcia, H.; Sousa, A. F.; Guerreiro, M.; Duarte, F. J. S.; Freire, C. S. R.; Calhorda, M. J.; Silvestre, A. J. D.; Kunz, W.; Rebelo, L. P. N.; Silva Pereira, C., Unveiling the dual role of the cholinium hexanoate ionic liquid as solvent and catalyst in suberin depolymerisation. *RSC Advances* **2014,** *4* (6), 2993-3002.https://doi.org/10.1039/C3RA45910A

37.   Garcia, H.; Ferreira, R.; Petkovic, M.; Ferguson, J. L.; Leitão, M. C.; Gunaratne, H. Q. N.; Seddon, K. R.; Rebelo, L. P. N.; Silva Pereira, C., Dissolution of cork biopolymers in biocompatible ionic liquids. *Green Chem.* **2010,** *12* (3), 367-369.https://doi.org/10.1039/B922553F

38.   Tran, T. K. N.; Colomines, G.; Nourry, A.; Pilard, J.-F.; Deterre, R.; Leroy, E., Hydroxyl telechelic natural rubber-based polyurethane: Influence of molecular weight on non-isothermal cure kinetics. *Thermochim. Acta* **2015,** *620*, 51-58.https://doi.org/10.1016/j.tca.2015.10.006

cutin monomers batch composition	%	(s.d.)
p-coumaric acid	1.8	(0.3)
16-hydroxy-hexadecanoic acid	2.7	(0.4)
16,9(10)-dihydroxyhexadecanoic acid	92.2	(2.3)
Hexadecane-1,16-dioic acid	0.4	(0.03)
7/8-hydroxy hexadecan-1,16-dioic acid	2.9	(1.2)

Supplemental Table 1 – Composition of the hydroxy-fatty acid fraction extracted from tomato cutin from industrial tomato peels

Value are means (standard deviation) of three experiments

665
666